workup. After evaporation of the solvent the residue was chromatographed through a silica column, with hexane as eluent. The first compound to be eluted was **30** (93 mg, 60%): deep-red crystals (from ether–MeOH) mp 190–195 °C dec; IR (CCl_4) 2060, 2025, 1990, 1915 cm^{-1}; ^1H NMR (300 MHz, C_6D_6) δ 8.36 (s, 1 H), 8.25 (s, 1 H), 7.48 (d, J = 1 Hz, 1 H), 7.34 (d, J = 1 Hz, 1 H), 7.28 (d, J = 0.7 Hz, 1 H), 6.92 (d, J = 0.8 Hz, 1 H), 0.339 (s, 9 H), 0.332 (s, 9 H), 0.328 (s, 9 H), 0.294 (s, 9 H); ^{13}C NMR (62.5 MHz, $CDCl_3$, 25 °C) δ 216.6, 209.2 (b), 207.2 (b), 158.0 (J_{CH} = 160 Hz), 152.7, 150.4, 150.0, 149.8, 148.4, 147.9, 147.1, 146.9, 143.1, 142.3, 132.9 (J_{CH} = 157 Hz), 132.4 (J_{CH} = 167 Hz), 126.9, 126.1 (J_{CH} = 161 Hz), 125.8 (J_{CH} = 162 Hz), 125.3, 110.9 (J_{CH} = 165 Hz), 2.1 ($J_{CH_3} = J_{C'H_3}$ = 119 Hz), 1.7 ($J_{CH_3} = J_{C'H_3}$ = 120 Hz); ^{13}C NMR ($CDCl_3$, −20 °C, CO region) δ 216.9 (intense), 209.7, 207.5, 207.1; MS, m/e (rel intensity) 794 (M^+, 31), 710 (33), 682 (51), 654 (48), 626 (100), 516 (23), 313 (40), 83 (21), 73 (81). Anal. Calcd for $C_{36}H_{42}Fe_2O_6Si_4$: C, 54.41; H, 5.33; Fe, 14.05. Found: C, 54.00; H, 5.51; Fe, 13.2.

Next to be eluted was a mixture of **30** and **33a** (19 mg, 60:40 from NMR), followed by pure **33a** (24 mg, 13%): red crystals (from hexane), mp 125–140 °C dec; IR (hexane) 2065, 2048, 2025, 1998, 1985, 1975 cm^{-1}; ^1H NMR (300 MHz, C_6D_6) δ 7.45 (d, J = 0.8 Hz, 1 H), 7.29 (d, J = 0.8 Hz, 1 H), 7.19 (d, J = 0.8 Hz, 1 H), 6.48 (d, J = 0.8 Hz, 1 H), 4.24 (s, 1 H), 3.71 (s, 1 H), 0.38 (s, 9 H), 0.37 (s, 9 H), 0.35 (s, 9 H), 0.31 (s, 9 H); ^{13}C NMR (62.5 MHz, $CDCl_3$) δ 212.4 (intense), 210.6, 209.8, 208.7, 208.3 (intense), 175.3, 155.5, 151.6, 150.5, 149.8, 149.5, 147.6, 145.7, 131.4 (J_{CH} = 166 Hz), 129.0, 126.1 (J_{CH} = 162 Hz), 125.9 (J_{CH} = 161 Hz), 118.6, 110.1 (J_{CH} = 166 Hz), 105.5, 103.1, 81.6 (J_{CH} = 164 Hz), 61.5 (J_{CH} = 160 Hz), 2.09 ($J_{CH_3} = J_{C'H_3}$ = 119 Hz), 174 (J_{CH_3} = 120 Hz), 1.59 (J_{CH_3} = 120 Hz). Anal. Calcd for $C_{39}H_{42}Fe_3O_9Si_4$: C, 50.12; H, 4.53; Fe, 17.92. Found: C, 50.21, H, 4.93; Fe, 18.0.

On further elution an orange solid of impure **35** (35 mg) was obtained, which was subjected to HPLC purification [reverse phase, CH_3CN–CH_2Cl_2 (80:20) as eluent] to give **35** (22 mg, 14%): orange solid, mp 150–170 °C dec; IR (CCl_4) 2050, 2010, 1990, 1960 cm^{-1}; ^1H NMR (300 MHz, C_6D_6) δ 7.52 (s, 4 H), 4.51 (s, 2 H), 0.29 (s, 36 H); ^1H NMR (300 MHz, acetone-d_6) δ (20 °C) 7.50 (s, 4 H), 5.53 (s, 2 H), 0.36 (s, 36 H); δ (−90 °C) 7.53 (s, 4 H), 5.66 (s, 2 H), 0.30 (s, 36 H); ^{13}C NMR (62.5 MHz, $CDCl_3$) δ 212.8, 148.4, 144.6, 125.8 (J_{CH} = 161 Hz), 68.8, 58.2 (J_{CH} = 179 Hz), 2.2 (J_{CH_3} = 120 Hz); MS m/e (rel intensity) 794 (M^+, 0.1), 710 (1), 654 (1), 626 (4), 598 (10), 570 (17), 514 (100), 499 (5), 411 (5), 387 (6), 207 (15), 97 (7), 86 (9), 73 (69), 57 (19). Anal. Calcd for $C_{36}H_{42}Fe_2O_6Si_4$: C, 54.41; H, 5.33; Fe, 14.05. Found: C, 53.97; H, 5.57; Fe, 13.8.

The next compound to be eluted during the HPLC purification of **35** was **36** (1.5 mg, 1%): brown solid; IR (CCl_4) 2030, 1967 cm^{-1}; ^1H NMR (300 MHz, C_6D_6) δ 7.63 (s, 2 H), 7.43 (s, 2 H), 6.36 (s, 2 H), 0.29 (s, 18 H), 0.27 (s, 18 H); MS, m/e (rel intensity) 654 (M^+, 0.4), 598 (16), 570 (28), 514 (100), 499 (6), 442 (13), 411 (6), 387 (7), 97 (15), 83 (13), 73 (87), 57 (32).

Preparation of Ketone 32 by Oxidation of 30. A solution of $FeCl_3 \cdot 6H_2O$ (1 g) in EtOH (5 mL) was added to a suspension of **30** (43 mg, 0.08 mmol) in EtOH (20 mL). The mixture was stirred for 3 days at room temperature, and the resulting orange solution was subjected to water–hexane workup. Evaporation of the solvent gave **32** (29 mg, 100%): red needles (from ether–EtOH), mp 204 °C; IR (CCl_4) 2960, 1715, 1600, 1255, 1160, 1100, 1060, 1020, 850 cm^{-1}; ^1H NMR (300 MHz, $CDCl_3$) δ 7.80 (s, 1 H), 7.62 (s, 1 H), 7.06 (d, J = 0.9 Hz, 1 H), 7.04 (d, J = 0.9 Hz, 1 H), 6.99 (d, J = 1 Hz, 1 H), 6.93 (d, J = 0.9 Hz, 1 H), 0.39 (s, 9 H), 0.36 (s, 9 H), 0.33 (s, 9 H), 0.325 (s, 9 H); ^{13}C NMR (62.5 MHz, $CDCl_3$) δ 194.1, 160.4, 155.0, 153.2, 150.4, 148.6 (b), 148.5, 148.1, 147.6, 142.1, 133.4, 131.9, 129.2 (J_{CH} = 160 Hz), 125.4 (J_{CH} = 158 Hz), 123.6 (J_{CH} = 161 Hz), 123.1 (J_{CH} = 161 Hz), 113.0 (J_{CH} = 167 Hz), 110.5 (J_{CH} = 165 Hz), 2.08 (J_{CH_3} = 119 Hz), 2.06 (J_{CH_3} = 119 Hz), 1.95 (J_{CH_3} = 119 Hz), 1.84 (J_{CH_3} = 119 Hz); MS, m/e (rel intensity) 542 (M^+, 57), 527 (7), 511 (5), 73 (100), 57 (6); HRMS calcd for $C_{31}H_{42}OSi_4$ 542.2313, found 542.2333.

Acknowledgment. This work was supported by NIH-CA20713. G.H.H. was on sabbatical leave from the University of Kuwait (1982-1983). H.M. was a C.N.R.S. (France) postdoctoral associate (1983–1984). K.P.C.V. was a Camille and Henry Dreyfus Teacher-Scholar (1978–1983).

Supplementary Material Available: For compounds **5** and **28**, tables of positional and thermal parameters and their estimated standard deviations, general temperature factor expressions, B's, and listings of observed and calculated structure factors (51 pages). Ordering information is given on any current masthead page.

Cation–Anion Interaction in the [Na-kryptofix-221][$W(CO)_5O_2CH$] Derivative and Its Relevance in Carbon Dioxide Reduction Processes

Donald J. Darensbourg* and Magdalena Pala

Contribution from the Department of Chemistry, Texas A&M University, College Station, Texas 77843. *Received February 22, 1985*

Abstract: The structure of [Na-kryptofix-221][$W(CO)_5O_2CH$] has been determined by X-ray crystallography and shown to exhibit a novel strong contact ion pairing between the uncoordinated oxygen of the formate ligand with the cryptand-encapsulated sodium cation. The compound crystallizes in the triclinic space group $P\bar{1}$ with cell dimensions a = 10.221 (2) Å, b = 10.845 (2) Å, c = 12.779 (2) Å, α = 87.93 (1)°, β = 89.47 (1)°, and γ = 82.99 (1)°. The most significant structural aspect is that the distance between the formate's distal oxygen atom and sodium (2.388 (9) Å) is the shortest Na–O bond distance in the cation's coordination sphere. Although this ion pairing persists for uncomplexed sodium cations in tetrahydrofuran solution, the cryptand-encapsulated species exists as a solvent-separated or free-ion pair in solution. Similar solution behavior is observed for the acetatotungsten pentacarbonyl anionic derivative. In addition, the $CH_3CO_2W(CO)_5^-$ anion, in the presence of 18-crown-6 complexed Na^+, displays a solution structure approximating that of the anion in the existence of the uncomplexed Na^+ cation. Consistent with these solution structures, the rate of reaction of carbon dioxide with $CH_3W(CO)_5^-$ to provide $CH_3CO_2W(CO)_5^-$ is enhanced by a factor of 10 in the presence of Na^+ or $Na(18\text{-crown-}6)^+$ over that carried out with the non-interacting PPN^+ (bis(triphenylphosphine)iminium cation) or Na-kryptofix-221$^+$. These rate accelerations are attributed to a cation stabilization of the incipient carboxylate during the carbon dioxide insertion process.

Alkali metal interactions with carbon dioxide are prevalent in chemistry associated with the reactivity of this C_1 molecule at transition-metal centers. For example, in the d^8 complex, [Co(pr-salen)K$(CO)_2$THF]$_n$, the CO_2 is bonded to the cobalt atom via the C functionality and simultaneously O bonded to two different K^+ ions.[1,2] Maher and Cooper[3] have shown that W-

0002-7863/85/1507-5687$01.50/0

$(CO)_5^{2-}$ can effect the disproportionation of CO_2 to metal-bound carbon monoxide by a pathway involving the intermediacy of species **1**.[4] A significant rate enhancement for the insertion of

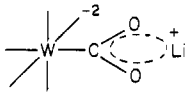

1

carbon dioxide into the tungsten–methyl bond was noted in the presence of alkali metal counterions[5,6] although no spectral evidence was observed for interaction of the alkali metal counterions with either the anionic metal substrate or free CO_2 in solution. We envisage the transition state for these processes to result from a concerted attack of the nucleophilic $CH_3W(CO)_5^-$ substrate on the electrophilic carbon or carbon–oxygen center of CO_2, with the alkali metal counterion serving to neutralize the negative charge which builds up on the distal oxygen atom of the incipient carboxylate ligand.

Tight ion pairing is noted between the ensuing metal carboxylate and the alkali metal ion to such an extent that the carboxylate is subsequently displaced from the metal center. This process is analogous to the reaction of these derivatives with methyl iodide to produce organic esters. Hence, in order to afford stable carboxylate derivatives from the reaction of CO_2 and anionic metal alkyls, a large noninteracting cation (e.g., PPN^+) is required. Inclusion complexes in which the alkali metal ion is contained inside a macropolycyclic ligand (e.g., a cryptand) offer an alternative method for isolating anions and cations.[7] Cryptands are generally much more effective than crown ethers in performing this task.[8] For example, in an instance of relevance to this correspondence, the solid-state structure of [Na-kryptofix-221][$Cr(CO)_5SH$][9] displays *no* anion–cation interactions, whereas significant Na–O(carbonyl) interaction is observed in [Na(18-crown-6)][$W(CO)_5SH$].[10]

We have synthesized the $W(CO)_5O_2CH^-$ complex with the [Na-kryptofix-221]$^+$ counterion, and herein we describe the X-ray structure of this derivative, where a novel strong contact ion pairing is observed between the uncoordinated oxygen atom of the formate ligand and the sodium ion. In addition, the solution structure and reactivity of this species and its acetato analogue are reported in efforts to evaluate the importance of this type of interaction during carbon dioxide insertion processes.

Experimental Section

All manipulations were carried out either in an argon drybox or on a double manifold Schlenk vacuum line, using tetrahydrofuran which was dried by distillation from sodium benzophenone ketyl under nitrogen. $W(CO)_6$ was purchased from Strem Chemicals, Inc., and methyl tosylate was acquired from Aldrich. Kryptofix-221 (4,7,13,16,21-pentaoxa-1,10-diazabicyclo[8.8.5]tricosane) was supplied by Parish Chemicals, Provo, UT. $W(CO)_5NMe_3$ was prepared from $W(CO)_6$ and $NMe_3O\cdot 2H_2O$ by the reported procedure.[11] Carbon monoxide enriched to 98.7% in ^{13}C was obtained from Mound Laboratories, Miamisburg, OH. Infrared spectra were recorded on either a Perkin-Elmer 283B or an IBM FTIR/85 spectrometer. Proton and ^{13}C NMR spectra were determined on a Varian XL-200 spectrometer.

Preparation of [Na-kryptofix-221][$W(CO)_5O_2CH$]. This complex was prepared by our published procedure from [Na-kryptofix-221][$W(CO)_5H$] and carbon dioxide.[12] Crystals suitable for X-ray analysis were grown at a temperature below 0 °C by layering hexane on a tetrahydrofuran solution of the complex.

Preparation of [Na-crypt-221][$W(CO)_5CH_3$]. The sodium naphthalenide solution, prepared from 0.425 g (3.30 mmol) of naphthalene and excess sodium in 30 mL of THF, was added dropwise to a 100-mL Schlenk flask containing 20 mL of a THF solution of $W(CO)_5NMe_3$ (0.437 g = 1.14 mmol) (cooled in a dry ice–acetone bath) until the mixture turned a deep red with a blue tint. Methyl tosylate (0.3 mL or ≈1.9 mmol) was then added and the mixture stirred for 20 min at −78 °C. After filtration through Celite under N_2 1.0 mL of a 1.1 M cryptofix-221 solution in THF was added to the filtrate which was stirred for 48 h at room temperature while protected from light. A cloudy yellow-orange solution was obtained, which was filtered twice through Celite under N_2. Upon precipitation with hexane, 0.31 g of the solid orange product was obtained (39 mol % yield). The infrared spectrum in THF had three bands at 2029 vw, 1883 vs, 1835 m [lit.[13] 2036 w, 1926 w, 1887 s, 1848 m]. ^1H NMR (CD_2Cl_2): δ −0.8 (s, 3 H), 2.6 (m, 11 H), 3.5 (m, 11 H), 3.6 (s, 8 H).

Reactions of [PPN][$W(CO)_5CH_3$] and [Na-crypt][$W(CO)_5CH_3$] with CO_2. These reactions were carried out in a 300-mL Parr reactor on ca. 5×10^{-3} M solutions of tungsten complexes in THF. The reactor vessel was evacuated, and the metal complex solution prepared under N_2 was transferred through a cannula. The system was then pressurized with CO_2 to 500 psi and stirred at room temperature. Samples were withdrawn every 20–30 min into the capped vials and analyzed by means of infrared spectroscopy. The progress of the reaction was followed by monitoring the disappearance of the band at 1883 cm^{-1} (E mode ν_{CO} vibration) in the starting material.

Reactions of [PPN][$W(CO)_5O_2CH$] and [Na-crypt][$W(CO)_5O_2CH$] with ^{13}CO. Tetrahydrofuran solutions of the tungsten formate complexes (ca. 1.6×10^{-2} M) were placed under a ^{13}CO atmosphere and stirred at room temperature. The progress of the $^{12}CO/^{13}CO$ exchange reaction was monitored by means of IR spectroscopy. Both cases exhibited similar rates of exchange resulting in complete ^{13}CO enrichment within 24 h.

X-ray Crystallographic Study of [Na-kryptofix-221][$W(CO)_5O_2CH$].[14] Data Collection and Reduction. An orange parallelepiped crystal of $C_{22}H_{33}NaN_2O_{12}W$ having approximate dimensions of 0.10 × 0.30 × 0.20 mm was mounted in a glass capillary in a random orientation. Preliminary examination and data collection were performed with Mo Kα radiation (γ = 0.71073 Å) on an Enraf-Nonius CAD4 computer controlled κ axis diffractometer equipped with a graphite crystal, incident beam monochromator.

Cell constants and an orientation matrix for data collection were obtained from least-squares refinement, using the setting angles of 19 reflections in the range $6 < \theta < 7°$, measured by the computer-controlled diagonal slit method of centering. As a check on crystal quality, ω scans of several intense reflections were measured; the width at half-height was 0.31° with a takeoff angle of 2.8°, indicating moderate crystal quality. There were no systematic absences; the space group was determined to be $P\bar{1}$ (No. 2).

The data were collected at a temperature of 23 ± 1 °C with use of the ω–θ scan technique. A total of 3848 reflections were collected, of which 3661 were unique. As a check on crystal and electronic stability, three representative reflections were measured every 33 min. The intensities of these standards remained constant within experimental error throughout data collection. No decay correction was applied.

Structure Solution and Refinement. The structure was solved by using the Patterson heavy-atom method which revealed the position of the W atom. The remaining atoms were located in a succeeding difference Fourier synthesis. Hydrogen atoms were not included in the calculations. The structure was refined in full-matrix least-squares analysis, where the function minimized was $\sum w(|F_o| - |F_c|^2)$ and the weight w is defined as $4F_o^2/\sigma^2(F_o^2)$.

Scattering factors were taken from Cromer and Waber.[15] Anomalous dispersion effects were included in F_c;[16] the values for $\Delta f'$ and $\Delta f''$ were those of Cromer.[17] Only the 2580 reflections having intensities greater than 3.0 times their standard deviation were used in the refinements. The final cycle of refinement included 344 variable parameters and converged

(1) Fachinetti, G.; Floriani, C.; Zanazzi, P. F. *J. Am. Chem. Soc.* **1978**, *100*, 7405.
(2) Gambarotta, S.; Arena, F.; Floriani, C.; Zanazzi, P. F. *J. Am. Chem. Soc.* **1982**, *104*, 5082.
(3) Maher, J. M.; Cooper, N. J. *J. Am. Chem. Soc.* **1980**, *102*, 7606.
(4) Maher, J. M.; Lee, G. R.; Cooper, N. J. *J. Am. Chem. Soc.* **1982**, *104*, 6796.
(5) Darensbourg, D. J.; Rokicki, A. *J. Am. Chem. Soc.* **1982**, *104*, 349.
(6) Darensbourg, D. J.; Kudaroski, R. A. *Adv. Organomet. Chem.* **1983**, *22*, 129.
(7) Parker, D. *Adv. Inorg. Chem. Radiochem.* **1983**, *27*, 1.
(8) Lehn, J. M. *Acc. Chem. Res.* **1978**, *11*, 49.
(9) Darensbourg, D. J.; Rokicki, A.; Kudaroski, R. *Organometallics* **1982**, *1*, 1161.
(10) Cooper, M. K.; Duckworth, P. A.; Henrick, K.; McPartlin, M. *J. Chem. Soc., Dalton Trans.* **1981**, 2357.
(11) Cooper, N. J.; Maher, J. N.; Beatty, R. P. *Organometallics* **1982**, *1*, 215.
(12) Darensbourg, D. J.; Rokicki, A. *Organometallics* **1982**, *1*, 1685.
(13) Casey, C. P.; Polichnowski, S. W. *J. Am. Chem. soc.* **1978**, *100*, 7567.
(14) These services were performed by the crystallographic staff of Molecular Structure Corp.: Dr. M. W. Extine, Dr. P. N. Swepston, Dr. J. M. Troup, and B. B. Warrington.
(15) Cromer, D. T.; Waber, J. T. "International Tables for X-ray Crystallography"; Kynoch Press: Birmingham, England, 1974; Vol. IV, Table 2.2B.
(16) Ibers, J. A.; Hamilton, W. C. *Acta Crystallogr.* **1964**, *17*, 781.
(17) Cromer, D. T. "International Tables for X-ray Crystallography"; Kynoch Press: Birmingham, England, 1974; Vol. IV, Table 2.3.1.

Table I. Crystallographic Summary

A. Crystal Data	
formula	$C_{22}H_{33}NaN_2O_{12}W$
fw	724.35
cryst dimens, mm	0.10 × 0.30 × 0.20
space group	$P\bar{1}$
lattice constants	
a, Å	10.221 (2)
b, Å	10.845 (2)
c, Å	12.779 (2)
α, deg	87.93 (1)
β, deg	89.47 (1)
γ, deg	82.99 (1)
V, Å^3	1405.0
Z	2
P_{calcd}, g/cm^3	1.71
B. Intensity Measurements	
instrument	Enraf-Nonius CAD4 diffractometer
radiation	graphite monochromated Mo Kα (λ = 0.71073 Å)
scan type	ω–θ
scan rate, deg/min	2–20 (in ω)
scan width, deg	0.9 + 0.350 tan θ
max 2θ, deg	45.0
no. of refletns measd	3848 total, 3661 unique
corrctns	Lorentz–polarization empirical absorption (from 0.81 to 1.00)
μ cm^{-1}	44.4
C. Structure Solution and Refinement	
solutn	Patterson method
hydrogen atoms	not included
refinement	full-matrix least squares
minimization function	$\sum w(\|F_o\| - \|F_c\|)^2$
least-squares weights	$4F_o^2/\sigma^2(F_o^2)$
"ignorance" factor	0.050
anomalous dispersion	all non-hydrogen atoms
reflctns included	2580 with $F_o^2 > 3.0\sigma(F_o^2)$
parameters refined	344
unweighted agreement factor[a]	0.047
weighted agreement factor[b]	0.055
esd of observn of unit weight	1.47
convergence largest shift	0.01σ
high peak in final diff map, e/Å^3	1.54 (14)

[a] $R_1 = \sum||F_o| - |F_c||/\sum|F_o|$. [b] $R_2 = [\sum w(|F_o| - |F_c|)^2/\sum wF_o^2]^{1/2}$.

(largest parameter shift was 0.01 times its esd) with unweighted and weighted agreement factors of 0.047 and 0.055, respectively. The standard deviation of an observation of unit weight was 1.47. The highest peak in the final difference Fourier had a height of 1.54 e/Å^3 with an estimated error based on ΔF[18] of 0.14 and was located in the vicinity of the W atom (1.31 Å). The formate H atom was not located in the final difference Fourier synthesis. Plots of $\sum w(|F_o| - |F_c|)^2$ vs. $|F_o|$, reflection order in data collection, sin θ/λ, and various classes of indices showed no unusual trends.

All calculations were performed on a PDP-11/60 based TEXRAY[19] system, which includes the Enraf-Nonius SDP and proprietary crystallographic software of Molecular Structure Corp.

Results and Discussion

Crystal and Molecular Structure of [Na-kryptofix-221][W(CO)$_5$O$_2$CH]. The final atomic coordinates and thermal parameters are collected in Table II. Figure 1 presents a perspective view of the complex structure and defines the atomic numbering scheme employed. Interatomic distances and angles, both for anion and cation, are provided in Tables III and IV.

It is clear from Figure 1 that the complex contains a monodentate formate ligand which is oriented such as to place its uncoordinated oxygen atom in the direction of sodium encapsulated in the cryptofix-221 framework. The disposition of the ligands about the tungsten atom is that of a regular octahedron. The average W–C(eq) distance is 2.037 (13) Å while the axial W–C bond length is considerably shorter at 1.911 (15) Å. Hence, the

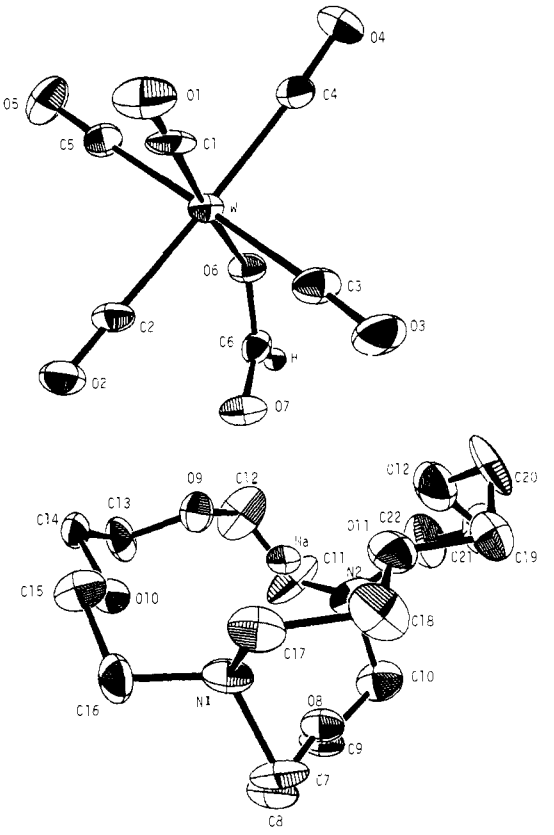

Figure 1. ORTEP drawing and numbering scheme for [Na-kryptofix-221][W(CO)$_5$O$_2$CH].

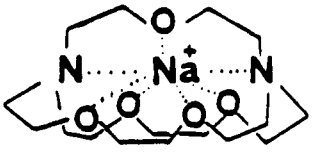

Figure 2. Structure of the cation [Na·crypt-221].$^+$

formate ligand, situated 2.216 (15) Å from the tungsten metal center, exerts a sizable trans effect. The difference in axial vs. equatorial metal–carbon bond lengths is 0.126 Å, which is larger than previously reported values in group 6 metal carbonyls[36] containing carboxylic ligands.[12,20-22] For instance, in W(CO)$_5$O$_2$CCH$_3^-$ this difference is 0.087 Å,[22] in Cr(CO)$_5$O$_2$CCF$_3^-$ it is 0.080 Å, and in Mo(CO)$_5$O$_2$CCF$_3^-$ the difference between the equatorial and axial M–C distances is 0.073 Å.[20]

We now turn our attention to the most distinguished feature of the structure, i.e., the accessibility of the alkali metal cation. It is well established that alkali metal cations form very stable inclusion complexes with macrobicyclic cryptates in which the metal cation is contained within a three-dimensional intramolecular cavity.[23] For example, in [Na·crypt-221]SCN it was found that the cation is bound to all the heteroatoms of the ligand, i.e., the sodium ion is heptacoordinated.[24] The idealized structure is a bicapped tetragonal pyramid. The sodium ion occupies a central

(18) Cruikshank, D. W. J. *Acta Crystallogr.* **1949**, *2*, 154.
(19) TEXRAY is a trademark of Molecular Structure Corp. (1982).

(20) Cotton, F. A.; Darensbourg, D. J.; Kolthammer, B. W. S. *J. Am. Chem. Soc.* **1981**, *103*, 398.
(21) Cotton, F. A.; Darensbourg, D. J.; Kolthammer, B. W. S. *Inorg. Chem.* **1981**, *20*, 1287.
(22) Cotton, F. A.; Darensbourg, D. J.; Kolthammer, B. W. S.; Kudaroski, R. *Inorg. Chem.* **1982**, *21*, 1656.
(23) (a) Anderegg, G. *Helv. Chim. Acta* **1975**, *58*, 1218. (b) Lehn, J. M.; Simon, J. *Ibid.* **1977**, *60*, 141. (c) Kauffmann, E.; Lehn, J. M.; Sauvage, J. P. *Ibid.* **1976**, *59*, 1099. (d) Mei, E.; Popov, A. I.; Dye, J. L. *J. Am. Chem. Soc.* **1977**, *99*, 6532. (e) Lin, J. D.; Popov, A. I. *J. Am. Chem. Soc.* **1981**, *103*, 1981. (f) Kauffmann, E.; Dye, J. L.; Lehn, J.-M.; Popov, A. I. *J. Am. Chem. Soc.* **1980**, *102*, 2274.
(24) Mathieu, F.; Metz, B.; Moras, D.; Weiss, R. *J. Am. Chem. Soc.* **1978**, *100*, 4412.

Table II. Table of Positional and Thermal Parameters and Their Estimated Standard Deviations[a]

atom	x	y	z	β(1,1)	β(2,2)	β(3,3)	β(1,2)	β(1,3)	β(2,3)
W	0.07378 (6)	0.13841 (5)	0.25106 (5)	0.0107 (5)	0.00707 (4)	0.00747 (3)	−0.00032 (8)	0.00109 (7)	−0.00068 (6)
NA	0.4820 (4)	−0.2627 (4)	0.2491 (4)	0.0102 (5)	0.0082 (4)	0.0079 (4)	−0.0010 (8)	0.0009 (7)	−0.0005 (7)
O1	−0.2304 (9)	0.1526 (9)	0.2605 (9)	0.0126 (11)	0.0119 (10)	0.0189 (11)	−0.001 (2)	0.004 (2)	−0.005 (2)
O2	0.0717 (10)	−0.0724 (8)	0.0890 (9)	0.0198 (14)	0.0102 (10)	0.0151 (10)	0.001 (2)	−0.007 (2)	−0.007 (2)
O3	0.0817 (12)	−0.0791 (9)	0.4259 (8)	0.0307 (19)	0.0103 (10)	0.0128 (9)	0.002 (2)	0.010 (2)	0.007 (2)
O4	0.0368 (11)	0.3533 (9)	0.4137 (8)	0.0236 (16)	0.0134 (10)	0.0107 (8)	0.002 (2)	0.004 (2)	−0.011 (1)
O5	0.0331 (11)	0.3443 (10)	0.0700 (9)	0.0237 (16)	0.0165 (12)	0.0138 (10)	−0.004 (2)	−0.008 (2)	0.012 (2)
O6	0.2914 (8)	0.1310 (7)	0.2517 (7)	0.0096 (9)	0.0093 (8)	0.0104 (7)	−0.001 (1)	−0.001 (1)	−0.002 (1)
O7	0.3387 (9)	−0.0719 (8)	0.2336 (8)	0.0130 (11)	0.0091 (9)	0.0147 (9)	0.002 (2)	0.003 (2)	0.000 (2)
O8	0.5946 (8)	−0.4846 (8)	0.2681 (7)	0.0098 (9)	0.0102 (9)	0.0127 (8)	0.001 (2)	0.000 (2)	−0.002 (1)
O9	0.6158 (10)	−0.1465 (10)	0.1124 (8)	0.0193 (14)	0.0185 (13)	0.0089 (8)	−0.007 (2)	0.002 (2)	0.003 (2)
O10	0.4339 (10)	−0.2992 (9)	0.0464 (8)	0.0219 (15)	0.0110 (10)	0.0104 (8)	−0.003 (2)	−0.001 (2)	−0.001 (2)
O11	0.3230 (11)	−0.2978 (10)	0.3951 (8)	0.0210 (15)	0.0154 (12)	0.0117 (9)	0.003 (2)	0.008 (2)	−0.003 (2)
O12	0.5424 (13)	−0.1661 (13)	0.4239 (9)	0.0275 (19)	0.0261 (17)	0.0128 (10)	−0.001 (3)	−0.012 (2)	-0.011 (2)
N1	0.319 (1)	−0.4395 (9)	0.214 (1)	0.011 (1)	0.009 (1)	0.014 (1)	−0.004 (2)	0.005 (2)	−0.003 (2)
N2	0.747 (1)	−0.2795 (11)	0.289 (1)	0.010 (1)	0.013 (1)	0.016 (1)	−0.003 (2)	0.002 (2)	0.010 (2)
C1	−0.114 (1)	0.149 (1)	0.2579 (12)	0.018 (2)	0.004 (1)	0.0123 (12)	0.003 (2)	0.004 (3)	−0.002 (2)
C2	0.078 (1)	0.005 (1)	0.1444 (11)	0.014 (2)	0.006 (1)	0.0117 (12)	−0.002 (2)	−0.001 (2)	−0.002 (2)
C3	0.082 (1)	0.000 (1)	0.3659 (11)	0.015 (2)	0.009 (1)	0.0113 (12)	−0.003 (2)	0.007 (2)	0.002 (2)
C4	0.055 (1)	0.276 (1)	0.3581 (10)	0.012 (2)	0.010 (1)	0.0084 (10)	0.003 (2)	0.001 2)	0.000 (2)
C5	0.055 (1)	0.270 (1)	0.1347 (11)	0.014 (2)	0.008 (1)	0.0096 (11)	−0.004 (2)	0.000 (2)	0.001 (2)
C6	0.371 (1)	0.033 (1)	0.2454 (9)	0.010 (1)	0.013 (1)	0.0062 (9)	0.003 (2)	0.001 (2)	0.002 (2)
C7	0.389 (1)	−0.560 (1)	0.2541 (14)	0.014 (2)	0.006 (1)	0.0201 (18)	−0.001 (2)	−0.002 (3)	0.003 (3)
C8	0.529 (1)	−0.575 (1)	0.2192 (14)	0.015 (2)	0.008 (1)	0.0180 (17)	−0.001 (3)	−0.005 (3)	−0.005 (3)
C9	0.729 (1)	−0.498 (1)	0.2448 (13)	0.012 (2)	0.009 (1)	0.0148 (14)	0.006 (2)	0.002 (3)	−0.005 (2)
C10	0.793 (1)	−0.407 (2)	0.3115 (15)	0.013 (2)	0.018 (2)	0.0182 (18)	0.004 (3)	−0.009 (3)	0.002 (3)
C11	0.814 (2)	−0.234 (2)	0.2001 (16)	0.013 (2)	0.027 (2)	0.0250 (20)	0.001 (4)	0.000 (3)	0.033 (3)
C12	0.746 (1)	−0.126 (2)	0.1457 (17)	0.010 (2)	0.032 (3)	0.0232 (21)	−0.021 (3)	−0.003 (3)	0.022 (4)
C13	0.608 (2)	−0.178 (2)	0.0097 (11)	0.030 (3)	0.022 (2)	0.0058 (11)	−0.018 (4)	0.004 (3)	−0.002 (3)
C14	0.464 (2)	−0.188 (1)	−0.0112 (11)	0.032 (3)	0.011 (1)	0.0072 (11)	−0.010 (3)	−0.010 (3)	0.003 (2)
C15	0.300 (1)	−0.312 (1)	0.0472 (15)	0.011 (2)	0.014 (2)	0.0189 (18)	−0.003 (3)	0.000 (3)	0.004 (3)
C16	0.281 (2)	−0.436 (2)	0.0977 (12)	0.019 (2)	0.019 (2)	0.0091 (12)	−0.010 (3)	−0.010 (3)	0.002 (3)
C17	0.199 (1)	−0.400 (1)	0.2707 (14)	0.013 (2)	0.015 (2)	0.0157 (16)	−0.003 (3)	0.006 (3)	−0.004 (3)
C18	0.231 (2)	−0.387 (2)	0.3890 (14)	0.020 (2)	0.020 (2)	0.0149 (16)	−0.022 (3)	0.013 (3)	−0.006 (3)
C19	0.362 (2)	−0.283 (2)	0.4949 (13)	0.040 (4)	0.018 (2)	0.0093 (14)	−0.007 (5)	−0.008 (4)	−0.005 (3)
C20	0.431 (2)	−0.172 (2)	0.4967 (11)	0.031 (3)	0.034 (3)	0.0071 (10)	−0.007 (5)	0.013 (3)	−0.020 (3)
C21	0.660 (2)	−0.213 (2)	0.4650 (14)	0.022 (2)	0.027 (3)	0.0123 (14)	−0.008 (4)	−0.014 (3)	−0.003 (3)
C22	0.766 (2)	−0.201 (2)	0.3847 (14)	0.019 (2)	0.032 (3)	0.0142 (16)	−0.023 (4)	−0.010 (3)	−0.009 (4)

[a] The form of the anisotropic thermal parameter is the following: $\exp[-(\beta(1,1)h^2 + \beta(2,2)k^2 + \beta(3,3)l^a + b(1,2)hk + \beta(1.3)hl + \beta(2,3)^*kl)]$. Estimated standard deviations in the least significant digits are shown in parentheses.

Table III. Table of Bond Distances in Angstroms[a]

atom 1	atom 2	distance	atom 1	atom 2	distance	atom 1	atom 2	distance
W	C1	1.911 (15)	O9	C12	1.44 (2)	C7	C8	1.49 (2)
W	C2	2.024 (14)	O9	C13	1.372 (15)	C9	C10	1.54 (2)
W	C3	2.053 (13)	O10	C14	1.454 (14)	C11	C12	1.44 (2)
W	C4	2.052 (13)	O10	C15	1.388 (14)	C13	C14	1.51 (2)
W	C5	2.020 (13)	O11	C18	1.433 (15)	C15	C16	1.50 (2)
O1	C1	1.185 (14)	O11	C19	1.36 (2)	C17	C18	1.56 (2)
O2	C2	1.121 (13)	O12	C20	1.47 (2)	C19	C20	1.46 (2)
O3	C3	1.133 (13)	O12	C21	1.35 (2)	C21	C22	1.50 (2)
O4	C4	1.116 (12)	N1	C7	1.486 (14)	Na	O7	2.388 (9)
O5	C5	1.135 (13)	N1	C16	1.54 (2)	Na	O8	2.542 (8)
O6	C6	1.259 (13)	N1	C17	1.438 (15)	Na	O9	2.594 (9)
O7	C6	1.240 (13)	N2	C10	1.43 (2)	Na	O10	2.693 (9)
O8	C8	1.422 (13)	N2	C11	1.43 (2)	Na	O11	2.512 (10)
O8	C9	1.392 (13)	N2	C22	1.54 (2)	Na	O12	2.612 (11)

[a] Numbers in parentheses are estimated standard deviations in the least significant digits.

position in the ligand cage, giving a fully unipositive complex cation (Figure 2). Such encapsulated sodium cations have been found not to be interacting with anionic counterions.[9,24]

However, the cryptate ligands have been found to exhibit some degree of flexibility. For example, these macrobicyclic ligands are able to adapt their conformation and internal cavity to cations of fairly different dimensions. In the case of cryptofix-221 it may coordinate with Na^+, K^+, or Co^{+2}.[24,25] The preference of the cryptofix-221 ligand for sodium ion over potassium ion is not due to cavity size but to favorable entropy effects.[24] In the reported structure (Figure 1) the sodium cation is situated unsymmetrically in the ligand frame as a result of interaction with the very nucleophilic formate ligand on its anionic counterpart. Table V contains pertinent bond distances and angles for the symmetrically encircled sodium cations, thus providing non-interacting ion pairs' bonding parameters for comparison with the structure reported herein. The sodium–oxygen distances within the Na-kryptofix-221$^+$ cation of the title compound are longer than those reported in instances where there are no significant interactions with the counteranion.[9,24] The basal Na–O bond distances average 2.603 Å which is 0.231 and 0.113 Å longer than that seen in the [Na-kryptofix-221][$Cr(CO)_5SH$][9] and the [Na-kryptofix-221][SCN][24] complexes, respectively. Similarly, the apical Na–O distance is 0.153 and 0.096 Å longer than the corresponding distances in the chromium and thiocyanate complexes. This observation taken together with the smaller O_{apical}–Na–O_{basal} angles means that the sodium cation is situated close to the plane defined

(25) Darensbourg, M. Y. *Prog. Inorg. Chem.* **1985**, *33*, 221 and references therein.

Table IV. Table of Bond Angles in Degrees[a]

atom 1	atom 2	atom 3	angle	atom 1	atom 2	atom 3	angle	atom 1	atom 2	atom 3	angle
C1	W	C2	90.0 (5)	C11	N2	C22	110 (1)	O12	C20	C19	117 (1)
C1	W	C3	88.1 (5)	W	C1	O1	178 (1)	O12	C21	C22	109 (2)
C1	W	C4	85.9 (5)	W	C2	O2	175 (1)	N2	C22	C21	111 (1)
C1	W	C5	88.7 (5)	W	C3	O3	176 (1)	O7	Na	O8	169.2 (4)
C2	W	C3	87.9 (5)	W	C4	O4	175 (1)	O7	Na	O9	81.1 (3)
C2	W	C4	175.9 (5)	W	C5	O5	174 (1)	O7	Na	O10	88.2 (3)
C2	W	C5	90.1 (5)	O6	C6	O7	125 (1)	O7	Na	O11	80.4 (3)
C3	W	C4	92.6 (5)	N1	C7	C8	111 (1)	O7	Na	O12	81.5 (4)
C3	W	C5	176.2 (5)	O8	C8	C7	109 (1)	O8	Na	O9	107.3 (3)
C4	W	C5	89.2 (5)	O8	C9	C10	108 (1)	O8	Na	O10	89.7 (3)
C8	O8	C9	112.1 (9)	N2	C10	C9	114 (1)	O8	Na	O11	92.1 (3)
C12	O9	C13	115 (1)	N2	C11	C12	116 (2)	O8	Na	O12	102.7 (4)
C14	O10	C15	113 (1)	O9	C12	C11	112 (1)	O9	Na	O10	63.7 (3)
C18	O11	C19	113 (1)	O9	C13	C14	107 (1)	O9	Na	O11	159.8 (3)
C20	O12	C21	114 (2)	O10	C14	C13	106 (1)	O9	Na	O12	102.0 (4)
C7	N1	C16	115 (1)	O10	C15	C16	109 (1)	O10	Na	O11	123.6 (4)
C7	N1	C17	114 (1)	N1	C16	C15	110 (1)	O10	Na	O12	163.7 (4)
C16	N1	C17	106 (1)	N1	C17	C18	110 (1)	O11	Na	O12	67.2 (4)
C10	N2	C11	111 (1)	O11	C18	C17	108 (1)				
C10	N2	C22	111 (1)	O11	C19	C20	109 (1)				

[a] Numbers in parentheses are estimated standard deviations in the least significant digits.

Table V. Comparison of Pertinent Distances and Angles in [Na·crypt-221]$^+$ Cations[a]

	counterion in complex		
	W(CO)$_5$OCHO$^-$ [b]	Cr(CO)$_5$SH$^-$ [c]	SCN$^-$ [d]
	Distances		
av Na–O$_{basal}$	2.603	2.472	2.490
av Na–O$_{apical}$	2.542	2.389	2.446
av Na–N1	2.742	2.608	2.703
av Na–N2	2.744	2.592	2.591
av O$_{basal}$–O$_{basal}$ (the same chain)	2.813	2.744	
interchain	4.318	3.759	
	Angles		
O$_{ap}$–Na–O$_{bas}$	89.7	101.5	101.0
	92.1	104.9	104.9
	102.7	118.7	115.6
	107.3	121.2	121.4

[a] Distances in Å, angles in deg; for labeling see Figure 1. [b] This work. [c] Reference 9. [d] Reference 24.

by the basal oxygen atoms, i.e., it is attracted out of the cryptand cage by the anionic formate ligand. *In fact, the distance between the formate's distal oxygen atom and sodium (2.388 (9) Å) is the shortest Na–O bond distance in the cation's coordination sphere.* The metallic ion in [K-kryptofix-221][SCN] is also octacoordinated, where the nitrogen atom of the thiocyanate anion completes the coordination shell of the potassium ion.[24] In this instance the O$_{ap}$–K–O$_{bas}$ angle is much smaller than the corresponding parameter in the Na$^+$ analogue, having an average value of 86.2°.

Comparison of the interchain oxygen distances (4.318 Å in this instance vs. 3.759 Å in the chromium–thiol complex, i.e., a difference of 0.559 Å) confirms that one face of the cryptand cage is open with carbon atoms directed outside of the ring, enabling the carbonyl oxygen of the formate ligand to reside within the sodium's coordination sphere. Also the Na–N distances are longer in the reported complex (av. 2.74 Å vs. 2.60 and 2.65 Å in the Cr(CO)$_5$SH$^-$ and SCN$^-$ complexes), which is consistent with a more open cryptand conformation and the unsymmetrical location of the sodium ion within the cage.

The Solution Structure of [Na-kryptofix-221][W(CO)$_5$O$_2$CH]. The [Na-kryptofix-221][W(CO)$_5$O$_2$CH] complex exists in tetrahydrofuran solution as a solvent-separated ion pair or free ions, since no direct interaction between the sodium ion and the uncoordinated oxygen atom of the formate ligand was noted by ^{13}C NMR or ν_{CO} infrared spectroscopy.[25] That is, the [Na-kryptofix-221][W(CO)$_5$O$_2$CH] salt has the same solution spectral properties as [PPN][W(CO)$_5$O$_2$CH]. Table VI summarizes these

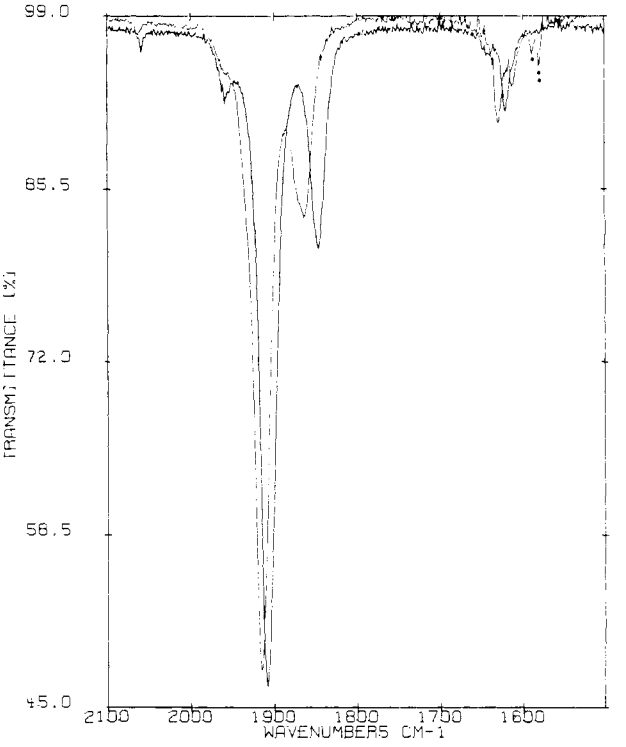

Figure 3. Infrared spectra in tetrahydrofuran solution. The **lighter** trace corresponds to [Na(THF)$_n$][W(CO)$_5$O$_2$CH] (produced by adding NaBPh$_4$ to [PPN][W(CO)$_5$O$_2$CH]) where the peak marked with a single asterisk at 1589 cm^{-1} is due to **PPN**$^+$ and that marked by a double asterisk at 1581 cm^{-1} is due to BPh$_4^-$. The **darker** trace is that of the [Na-kryptofix-221][W(CO)$_5$O$_2$CH] salt.

spectral data, along with comparable data for the [Na(THF)$_n$]$^+$ and [Na-18-crown-6]$^+$ salts (see Figure 3). Corresponding spectral data are provided as well in Table VI for the [PPN][W(CO)$_5$O$_2$CH] salt in the protic (hydrogen-bonding) solvent, methanol.

Interaction of the distal formate oxygen atom with Arrhenius (MeOH) or Lewis (Na$^+$) acids leads to a shift in the ν_{CO} vibrations to higher frequencies and a downfield displacement of the δ_{O_2CH} resonance.[26] Analogous spectral shifts have been reported for

(26) The asymmetric $\nu(CO)_2$ vibration shifts to lower frequency in the presence of MeOH; however, the addition of Na$^+$ ions results in two peaks in this region, one shifted to higher frequency and one to lower. At this point we are unable to offer an explanation for this observation. An analogous measurement of the acetate sample revealed only one band shifted to lower frequency.

Table VI. Infrared and ^{13}C NMR Spectral Data for the $W(CO)_5O_2CH^-$ Anion[a]

cation	ν_{CO}, cm^{-1}				δ_C		
	$A_1^{(2)}$	$A_1^{(1)}$	E	$\nu_{CO_2}^-$, (sym)	CO_{ax}	CO_{eq}	O_2CH
[Na-kryptofix-221]$^+$	2060	1848	1908	1622	205.7	201.3	167.5
[PPN]$^+$	2059	1846	1908	1621	205.0	200.2	167.4
							167.1
[Na-18-crown-6]$^+$	2060	1849	1911	1621, 1614			
[Na(THF)$_n$]$^+$	2064	1864	1915	1631, 1612			
[PPN]$^+$ in methanol	2017.5	1869	1927	1607			170.9

[a] Tetrahydrofuran solution.

the $RC(O)Fe(CO)_4^-$ (R = H, CH_3)[27] and its phosphine-substituted derivatives.[28] This highly basic property of the unbound oxygen atom of the carboxylate ligands in group 6 metal carbonyl species most likely accounts for their involvement in processes which appear to proceed via heterocyclic cleavage of dihydrogen.[29]

In an effort to examine possible differences in the solution reactivity of the $W(CO)_5O_2CH^-$ anion in the presence of encapsulated vs. uncomplexed sodium ions, we have chosen to investigate the most elementary reaction, i.e., the CO exchange process (eq 1). These derivatives, $W(CO)_5O_2CR^-$ (R = H, CH_3), have been shown to easily undergo CO ligand substitution by a variety of incoming ligands, e.g., ^{13}CO, phosphines, and phosphites.[22] This ligand substitutional process seems a natural choice

$$W(CO)_5O_2CH^- + n^{13}CO \rightarrow W(CO)_{5-n}(^{13}CO)_nO_2CH^- + n^{12}CO \quad (1)$$

based on past experiences. Namely, we have previously examined the effect on CO labilization of contact Na^+ ion interaction with the equatorial CO oxygen atoms in $HFe(CO)_4^-$.[30] Relative to the non-interacting PPN^+ cation, the uncomplexed sodium ion was found to dramatically accelerate CO dissociation, presumably labilizing those CO groups not involved in direct contact ion pairing with Na^+.

Consistent with the spectral solution data, the $[PPN]^+$ and [Na-kryptofix-221]$^+$ salts of $W(CO)_5O_2CH^-$ in THF both exhibited facile CO ligand exchange with atmospheric pressure of ^{13}CO at ambient temperature. By way of contrast, [Na(THF)$_n$][$W(CO)_5O_2CH$], which featured a tight-ion pair in THF solution, underwent analogous CO exchange reactions at a much slower rate.[31] Therefore the effect of neutralizing the negative charge on the formato ligand in $W(CO)_5O_2CH^-$ appears to render it much less CO labilizing.[32]

Hence, although the solid-state structure of [Na-kryptofix-221][$W(CO)_5O_2CH$] displays strong contact ion pairing between the encapsulated sodium ion and the distal oxygen of the formate ligand, *the solution structure and reactivity are indicative of solvent-separated ion pairs.* Lin and Popov have presented sodium-23 NMR data which suggest that, even when Na^+ is situated in the center of the cryptofix-221 ligand cage, weak interactions between Na^+ and solvent molecules can occur through the ligand's "open-face".[23e] The above type of interactions are either insufficient to have an effect on the reaction rates studied herein, or preferentially occur with the solvent (THF) as opposed to the metal-bound formate or carboxylate ligands.

Reactivity of [Na-kryptofix-221][$W(CO)_5O_2CH$] toward Carbon Dioxide. We have previously reported a significant rate enhancement for the insertion of CO_2 into the tungsten–methyl bond in the presence of alkali metal counterions.[5,6] Indeed this interaction of the alkali metal cation with the carboxylate ligand is so pronounced that it results in displacement of the carboxylate ligand by the solvent, tetrahydrofuran, which is subsequently replaced by CO (vide infra).

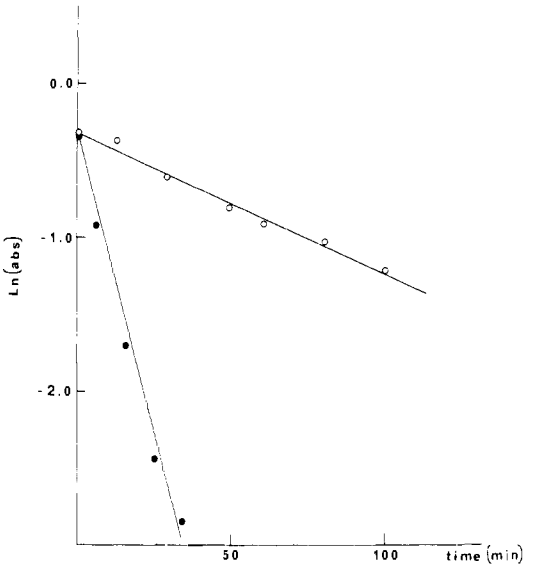

Figure 4. Representative kinetic plots of the CO_2 insertion reaction with $CH_3W(CO)_5^-$ at 500 psi in THF solvent at ambient temperature: (○) [Na-kryptofix-221]$^+$ salt, (●) [Na-18-crown-6]$^+$ salt.

Table VII. Cation Effect on the Rate of CO_2 Insertion into the $W-CH_3$ Bond in $W(CO)_5CH_3^-$ Derivatives[a]

cation	k_{obsd},[b] 10^4 s^{-1}
[Na-kryptofix-221]$^+$	1.53 (1.00)
PPN^+	2.08 (1.36)
Na^+	11.9 (7.78)
[Na-18-crown-6]$^+$	12.6 (8.24)

[a] Reactions carried out at 500 psi of CO_2 in THF in ambient temperature. [b] k_{obsd} is the pseudo-first-order rate constant. Relative rate data are listed in parentheses.

The reactivity of $W(CO)_5H^-$ toward carbon dioxide insertion is very facile even at low pressures of CO_2.[33] Hence, it is not readily feasible to measure the kinetic effect of alkali metal ions, in particular cryptand encapsulated alkali metal ions, on carbon dioxide insertion processes which provide the formato ligand. Therefore, we report here kinetic measurements of CO_2 insertion into the tungsten–methyl bond to afford tungsten carboxylate as a function of counterion (eq 2).

$$W(CO)_5CH_3^- + CO_2 \rightarrow W(CO)_5O_2CCH_3^- \quad (2)$$

Pseudo-first-order rate constants for the reaction defined by eq 2 are tabulated in Table VII. Whereas Figure 4 contains representative plots of the data employing in computing these rate constants. In a separate study, this process has been examined as a function of carbon dioxide pressure and shown to be first order both in metal alkyl substrate and carbon dioxide.[34] In this instance

(27) Collman, J. P.; Winter, S. R. *J. Am. Chem. Soc.* **1973**, *95*, 4089.
(28) Darensbourg, M. Y.; Burns, D. *Inorg. Chem.* **1974**, *13*, 2970.
(29) Darensbourg, D. J.; Ovalles, C. *J. Am. Chem. Soc.* **1984**, *106*, 3750.
(30) Darensbourg, M. Y.; Darensbourg, D. J.; Barros, H. L. C. *Inorg. Chem.* **1978**, *17*, 297.
(31) This process is somewhat complicated by the displacement of the formate ligand in the presence of Na^+ cations; however, it is clear that the rate of intermolecular carbon monoxide exchange is significantly retarded.
(32) We plan to investigate this phenomenon in detail, for there are several anionic metal carbonyl derivatives which contain CO-labilizing ligands capable of ion pairing with Lewis acids.
(33) Darensbourg, D. J.; Rokicki, A.; Darensbourg, M. Y. *J. Am. Chem. Soc.* **1981**, *103*, 3223.
(34) Darensbourg, D. J.; Hanckel, R. K.; Bauch, C. G.; Pala, M.; Simmons, D.; White, J. N., in press.

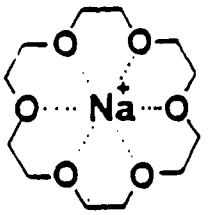

Figure 5. Structure of the cation [Na·18-crown-6]$^+$.

the carbon–carbon bond-forming process was investigated at high carbon dioxide pressure (500 psi) both as a matter of convenience and in order to minimize subsequent carboxylate displacement reactions which are prevalent in the presence of interacting alkali metal ions (eq 3). As can be readily seen in Table VII and

$$M(CO)_5O_2CCH_3^- + Na^+ \xrightarrow{THF} M(CO)_5THF + NaO_2CCH_3 \quad (3)$$

depicted in Figure 4, the cryptand-encapsulated sodium cation exhibits *no* effect on the rate of CO_2 insertion into the W–CH_3^- bond, i.e., the pseudo-first-order rate constant is quite similar to that noted when the non-interacting PPN^+ counterion was employed. This is not totally unexpected since no interaction in solution was observed between the once formed anionic metalloformate or -acetate derivatives and Na(kryptofix-221)$^+$ cation.

On the other hand, there is approximately a 10-fold increase in the rate of CO_2 insertion into $W(CO)_5CH_3^-$ in the presence of $Na(THF)_n^+$ or Na(18-crown-6)$^+$. In the crown ether species (Figure 5), the complex has two open faces which allow access to the anion.[35] Indeed in both the $Na(THF)_n^+$ and Na(18-crown-6)$^+$ derivatives perturbation of the carboxylate ligands by the Na^+ was noted by spectral measurements (Table VI). Concomitantly, more facile loss of the carboxylate ligand was observed during CO_2 insertion reactions involving these counterions. It is worthy of note here that spectroscopic studies have demonstrated that although the rate of cationic exchange in the $NaBPh_4$/18-crown-6/THF system is slow (two ^{23}Na resonances observed in excess Na^+ at −7.9 and −17.1 ppm), the exchange rate is highly dependent on the accompanying anion.[23e]

Acknowledgment. The financial support of this research by the National Science Foundation (Grant CHE 83-08281) is greatly appreciated. We thank J. Nicole White for experimental assistance in some aspects of these investigations.

Registry No. [Na-kryptofix-221][$W(CO)_5O_2CH$], 97860-74-7; [Na-crypt-221][$W(CO)_5CH_3$], 97877-24-2; [PPN][$W(CO)_5CH_3$], 62197-79-9; [PPN][$W(CO)_5O_2CH$], 36499-81-7; CO_2, 124-38-9; ^{13}CO, 1641-69-6.

Supplementary Material Available: A list of observed and calculated structure factors and a table of intermolecular contacts up to 3.8 Å (9 pages). Ordering information is given on any current masthead page.

(35) Interaction of this type have been noted previously, e.g., see ref 10.
(36) In this paper the periodic group notation is in accord with recent actions by IUPAC and ACS nomenclature committees. A and B notation is eliminated because of wide confusion. Groups IA and IIA become groups 1 and 2. The d-transition elements comprise groups 3 through 12, and the p-block elements comprise groups 13 through 18. (Note that the former Roman number designation is preserved in the last digit of the new numbering: e.g., III → 3 and 13.)

Characterization of Five-Coordinate Mono(imidazole)(porphinato)iron(III) Complexes

W. Robert Scheidt,*[1] David K. Geiger,[1] Young Ja Lee,[1] Christopher A. Reed,[2] and G. Lang*[3]

Contribution from the Departments of Chemistry, University of Notre Dame, Notre Dame, Indiana 46556, University of Southern California, Los Angeles, California 90089-1062, and the Department of Physics, Pennsylvania State University, University Park, Pennsylvania 16802.
Received March 4, 1985

Abstract: The preparation of two crystalline forms of [Fe(OEP)(2-MeHIm)]ClO_4 is described. Both crystalline forms have been characterized by X-ray structure determinations, and the five-coordinate group [Fe(OEP)(2-MeHIm)]$^+$ has been confirmed for both. One of the species has also been fully characterized by Mössbauer spectroscopy and temperature-dependent (6-299 K) magnetic susceptibilities. Mössbauer parameters (4.2 K, zero applied field, symmetric doublet) are ΔE_q = 1.39 and δ = 0.40 mm/s for the chloroform solvate. The effective spin is temperature-independent down to ~60 K (μ = 5.9–5.99 μ_B), falling off to 3.7 μ_B at 6 K. The complexes are best described as high-spin species. The temperature dependence of the susceptibility can be fit with a zero-field splitting constant of D = 12 cm^{-1} and weak intermolecular antiferromagnetic coupling ($-J$ = 0.8 cm^{-1}) between adjacent pairs of ions. The Mössbauer data (6-T applied field) are also consistent with these parameters. Crystal data for [Fe(OEP)(2-MeHIm)]ClO_4·$CHCl_3$ are monoclinic, a = 22.786 (6) Å, b = 15.028 (4) Å, c = 49.974 (13) Å, β = 101.70 (2)°, Z = 16, space group $C2/c$, 3933 observed data, and all measurements at 96 K. Crystal data for [Fe(OEP)-(2-MeHIm)]ClO_4·CH_2Br_2 are monoclinic, a = 15.059 (3) Å, b = 19.040 (4) Å, c = 15.093 (3) Å, β = 92.40 (1)°, Z = 4, space group $P2_1/n$, 8658 observed data, R_1 = 0.087, R_2 = 0.092, and all measurements at 100 K. Pertinent structural data are Fe–N_p = 2.038 (6) Å, Fe–N(2-MeHIm) = 2.068 (4) Å; the iron(III) ion is displaced 0.36 Å from the mean porphinato ligand plane (CH_2Br_2 solvate). Pertinent structural data for the chloroform solvate are Fe–N_p = 2.039 (28) Å, Fe–N(2-MeHIm) = 2.09 Å; the iron(III) ion is displaced 0.34 Å from the mean porphinato ligand plane. Both solvates share a common intermolecular π–π interaction between two [Fe(OEP)(2-MeHIm)]$^+$ units. This π–π complex formation is regarded as a significant factor in the isolation of monoligated species rather than the more common bis-ligated ferric complex.

The multiplicity of chemical functions for the hemoproteins continues to arouse curiosity. In attempting to understand how this is achieved in Nature, much attention has been given to the role of the axial ligand(s) in controlling the chemistry and/or the physical properties of the hemoproteins. An imidazole (histidine) residue is a common axial ligand for the heme in hemoproteins. Despite the frequent occurrence of histidine in hemoproteins, the synthetic chemistry of iron porphyrinates having a single imidazole[4]

(1) University of Notre Dame
(2) University of Southern California
(3) Pennsylvania State University

0002-7863/85/1507-5693$01.50/0